Mat. Res. Soc. Symp. Proc. Vol. 674 © 2001 Materials Research Society

Studies on Crystal Structure and Magnetic Scaling Behavior of Perovskite-Like $(La_{1-x}Pb_x)MnO_3$ System with $x = 0$ - 0.5

Ting-Sheng Huang, Chiung-Hsiung Chen and Ming-Fong Tai
Department of Physics, Chung Cheng University,
160 San-Hsing, Ming-Hsiung, Chia-Yi 621, Taiwan, R. O. C.

ABSTRACT

The magnetic critical behaviors in the perovskite-like $(La_{1-x}Pb_x)MnO_3$ series with $x = 0.0 \sim 0.5$ are studied by means of *dc* magnetic measurements. All the samples crystallize in the rhombohedral unit cell with a $R\bar{3}C$ space group ($a \sim 0.54$ nm and $c \sim 1.33$ nm). The detailed crystallographic parameters of all the samples are obtained by the refinements of the powder x-ray diffraction data using the Rietveld method. The substitution effect of Pb^{2+} ions on La^{3+} sites induces a mixed-valence state of Mn^{3+}/Mn^{4+} and enhances magnetic transition temperature in the $(La_{1-x}Pb_x)MnO_3$ system. The transition temperature T_C increases with the Pb content from 225 K as $x = 0$ to 355 K as $x = 0.5$. The canonical spin-glass behaviors in low fields and the scaling behaviors of magnetic physical quantities are clearly observed in all our samples. The values of the related critical exponents and the scaling functions of magnetic data are close to those of the conventional spin glass systems.

INTRODUCTION

The rich physical properties in the perovskite-like $(Ln_{1-x}A_x)MnO_3$ series (Ln = trivalent rare earths, A = divalent alkali metals, *e.g.* Ca, Sr, Ba, and Pb) have attracted many interests since the discoveries of the colossal magnetoresistance (CMR) effect [1,2]. Many anomalous phenomena, including high negative magnetoresistance ratio, metal-insulator transitions and anomalous lattice expansions *etc.*, are found in the vicinity of the critical point. Despite much efforts made, the nature of this magnetic critical behavior is still not clear. An extensive study of flux-growth single crystals of $(La_{1-x}Pb_x)MnO_3$ series with $0.2 \leq x \leq 0.4$ has been carried out by some groups [1,3-5]. The metallic conductivity was observed below the Curie transition point T_C and a negative magnetoresistance effect of ~ 20 % at $H = 1$ T was found in the vicinity of T_C. C. W. Serale *et al.* [3-5] suggested that a fully spin-polarized *d* band is involved in the ferromagnetic ordering process of the Pb-doping manganese. Very few researches have been working out on this system since 1970. In this paper we report the detailed studies of the crystal structure, magnetic properties and scaling behaviors of the perovskite-like $(La_{1-x}Pb_x)MnO_3$ manganese.

EXPERIMENTAL DETAILS

Samples $(La_{1-x}Pb_x)MnO_3$ with $x = 0$ - 0.5 were prepared using a conventional powder solid-state reaction method. Stoichoimetric amounts of high-purity La_2O_3, Pb_3O_4, and MnO_2 raw powders were homogenously mixed and completely ground, thus the mixed samples were fired to 1000 - 1300°C and hold at the same temperature for 12 hours. The heated samples were cooled to low temperature and removed, reground, and reheated at the same temperature for an addition 24 h. The processes were repeated at least three times until the samples are of a single

Table I. Selected crystallographic and magnetic parameters of $(La_{1-x}Pb_x)MnO_3$ samples with $x = 0 - 0.5$. Numbers in the parenthesis are errors of the least significant digit.

Pb content x	Crystal System: Trigonal, a hexagonal axes Space group: $R\bar{3}c$, $\alpha = \beta = 90°$, $\gamma = 120°$				Volume of unit cell	Magnetic transition point		Effective moment (μ_B)	
	a (Å)	c (Å)	d_x (g/cm^3)	R_{wp} (%)	V_{cell} (Å^3)	T_c (K)	θ_p (K)	μ_{FM}	μ_{PM}
0.0	5.5008(5)	13.276(6)	5.35	10.47	347.90(8)	225	240	3.35	4.59
0.1	5.5033(3)	13.293(4)	5.54	12.47	348.66(2)	271	293	3.48	5.65
0.2	5.5019(9)	13.293(3)	5.74	13.10	348.49(0)	275	270	3.44	4.78
0.3	5.5037(1)	13.334(6)	5.91	12.02	349.79(1)	350	341	3.19	5.17
0.4	5.5217(3)	13.404(3)	6.03	12.27	353.92(6)	358	347	3.20	5.43
0.5	5.4842(2)	13.383(0)	6.32	13.14	348.57(9)	355	353	3.15	5.41

phase. The thoroughly reacted powders were pressed into pellets during the last sintered process. All heated processes were progressed at ambient atmosphere and used warm-up and cooling rates of 300°C/h.

X-ray powder diffraction (XRD) data were collected with a Rigaku Rotaflex RTP500RC powder X-ray diffractometer using Cu $K\alpha$ radiation and a secondary graphite monochromator from 20° to 100° with a step size of 0.02° in $2\theta/\theta$ scanning mode and a counting rate of 5 sec/step. The XRD patterns were refined by a Riqas program based on the Rietveld analysis technique. Magnetic measurements were performed on using an Oxford MagLab magnetometer and a Bruck Vibrating Sample magnetometer (VSM) systems for $T < 300$ K and $T > 300$ K, respectively. The zero-field cooling (ZFC) and field cooling (FC) magnetization curves were carried out under various *dc* external fields H from 0 – 5 T. Isothermal magnetic hysteresis loops at various temperatures were also obtained in applied fields up to 5 T.

RESULTS AND DISCUSSION

XRD data of all the samples showed single-phase patterns, which are described well by an rhombohedral (trigonal) unit cell with space group $R\bar{3}c$ rather than an orthorhombic unit cell with space group *Pbnm*. Detailed crystallographic data extracted from the refinement results of XRD data were listed in tables I - III. The results show that there was almost no Pb lossing during the sample preparation procedures and the compositions of all atoms were consistent with the original stoichoimetries. Lattice parameters, Mn-O bond length and Mn-O-Mn bond angle as a function of the Pb content are drawn in figure 1. Lattice parameters a and c slightly vary as $x \leq 0.3$, then suddenly increas at $x \sim 0.4$, but slightly decrease again as $x = 0.5$, as shown in Figure 1(a). The bond length between Mn and O ions is found a small oscillating variation as $x < 0.4$, then abruptly becomes short as $x = 0.5$. The dependence of the bond angle of Mn-O-Mn on x is found an inverse variation. The change of the La/Pb ratio is not only to change the average ion radius $\langle r_A \rangle$ in the La/Pb sites, but also to affect the average radius of the transition metal ions $\langle r_{Mn} \rangle$ in the Mn^{3+}/Mn^{4+} site. In perovskite-structure oxides, the ionic radius of Pb^{2+} (1.49 Å) is larger smaller than that of La^{3+} (1.36Å), but the ionic radius of Mn^{4+} is 0.53 Å is smaller than that

of Mn^{3+} (0.645 Å). So it is possible that both the $<r_A>$ and the ratio of Mn^{4+}/Mn^{3+} increases with increasing x, however, $<r_{Mn}>$ decreases. As a result that the variation of the lattice constants *a* and *c* with the Pb content does not obey a simple linear relation of the Vegard's law. In addition, the chemical order or charge order may occur for certain special compositions such that allow to have very complex relations between the crystallographic parameters and the Pb content.

Table II. Summary of the room-temperature XRD refinements of $(La_{1-x}Pb_x)MnO_3$ samples with x = 0-0.5 using a Riqas program based on the Rietveld analysis technique. Numbers in the parenthesis are errors of the least significant digit.

Crystal System: Trigonal, hexagonal axes

Space group $R\bar{3}c$ (NO.167), $\alpha = \beta = 90°$, $\gamma = 120°$, Z = 6

Atomic positions: La/Pb (6a), Mn^{3+}/Mn^{4+} (6b), O (18e)

La/Pb (0.00, 0.00, 0.75), Mn^{3+}/Mn^{4+} (0, 0, 0), O (x, 0.00, 0.25)

Pb content	Ion	X	Y	Z	B	N
	La^{3+}	0	0	0.75	1.14	1.00
x = 0.0	Mn^{3+}	0	0	0	0.20	1.00
	O^{2-}	0.5567(1)	0	0.25	2.93	1.10
	La^{3+}	0	0	0.75	0.08	0.88
	Pb^{2+}	0	0	0.75	0.10	0.10
x = 0.1	Mn^{3+}	0	0	0	0.13	0.98
	Mn^{4+}	0	0	0	0.20	0.10
	O^{2-}	0.5512(4)	0	0.25	1.69	1.00
	La^{3+}	0	0	0.75	0.06	0.78
	Pb^{2+}	0	0	0.75	0.10	0.20
x = 0.2	Mn^{3+}	0	0	0	0.30	0.97
	Mn^{4+}	0	0	0	0.06	0.20
	O^{2-}	0.5540(5)	0	0.25	1.98	1.19
	La^{3+}	0	0	0.75	0.67	0.69
	Pb^{2+}	0	0	0.75	0.65	0.30
x = 0.3	Mn^{3+}	0	0	0	0.40	0.75
	Mn^{4+}	0	0	0	0.20	0.30
	O^{2-}	0.4552(4)	0	0.25	1.22	1.07
	La^{3+}	0	0	0.75	0.59	0.52
	Pb^{2+}	0	0	0.75	0.64	0.41
x = 0.4	Mn^{3+}	0	0	0	0.99	0.70
	Mn^{4+}	0	0	0	0.20	0.40
	O^{2-}	0.4618(7)	0	0.25	2.06	1.04
	La	0	0	0.75	0.26	0.49
	Pb	0	0	0.75	0.30	0.50
x = 0.5	Mn^{3+}	0	0	0	0.29	0.57
	Mn^{4+}	0	0	0	0.20	0.50
	O^{2-}	0.5355(4)	0	0.25	1.30	1.07

Table III. Bond angles of both Mn-O-Mn and O-Mn-O bonds and bond lengthsof Mn-O bond of $(La_{1-x}Pb_x)MnO_3$ samples with $x = 0$ - 0.5.

Sample	Mn-O-Mn Bond Angle (degrees)	O-Mn-O Bond Angle (degrees)	Mn-O Bond Length (Å)
$LaMnO_3$	161.77°	180° (91.27°)	1.9601
$La_{0.9}Pb_{0.1}MnO_3$	163.43°	180° (91.11°)	1.9573
$La_{0.8}Pb_{0.2}MnO_3$	162.54°	180° (91.17°)	1.9591
$La_{0.7}Pb_{0.3}MnO_3$	167.65°	180° (90.86°)	1.9544
$La_{0.6}Pb_{0.4}MnO_3$	168.51°	180° (90.67°)	1.9578
$La_{0.5}Pb_{0.5}MnO_3$	168.47°	180° (90.43°)	1.9463

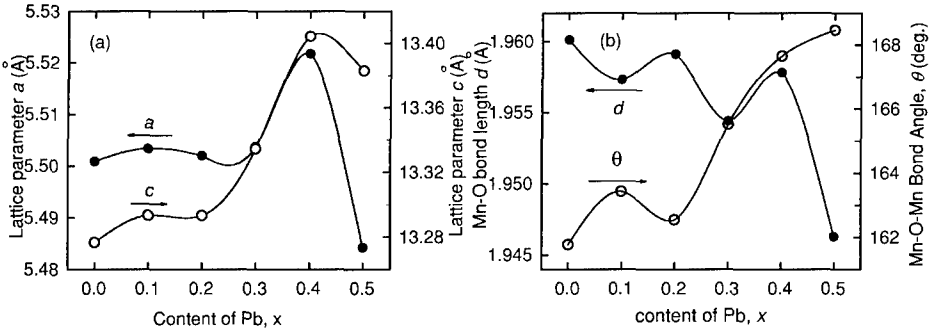

Figure 1. Lattice parameters a and c as a function of Pb contration x. (b) Dependence of Mn-O bond length and Mn-O-Mn Pb content. All lines are drawn to guide the eyes.

Some magnetic parameters of $(La_{1-x}Pb_x)MnO_3$ samples, including the ferromagnetic critical point T_C and Curie-Weiss transition temperature θ_p and effective magnetic moment per Mn site in FM and PM states, μ_{FM} and μ_{PM}, were determined from *dc* magnetization and inverse susceptibility versus temperature in an external field. These parameters are listed in table I. The substitution effect of Pb^{2+} ion on La^{3+} site in this system induces a mixed-valence state of Mn^{3+}/Mn^{4+} and enhances the ferromagnetic transition temperature. Although the dependence of transition temperature with x presents an oscillating variation, both T_C and θ_p trend to linearly increase with x, as shown in the inset plot of figure 2(a). The transition temperature T_C increases with the Pb content from 225 K as $x = 0$ to 355 K as $x = 0.5$, but an anomalous reduce at $x = 0.3$ Both curves are similar to the variation trend of Mn-O-Mn bond angle in figure 1(b). The effective magnetic moments per Mn site in both FM and PM states vary in the ranges of 3.3 ± 0.3 μ_B and 5.5 ± 0.5 μ_B, respectively. Based on the comparison between crystal parameters and magnetic parameters shown in figures 1 and 2, the variation trends of those magnetic quantities with the Pb doping apparently depends upon the results of the crystallographic variation.

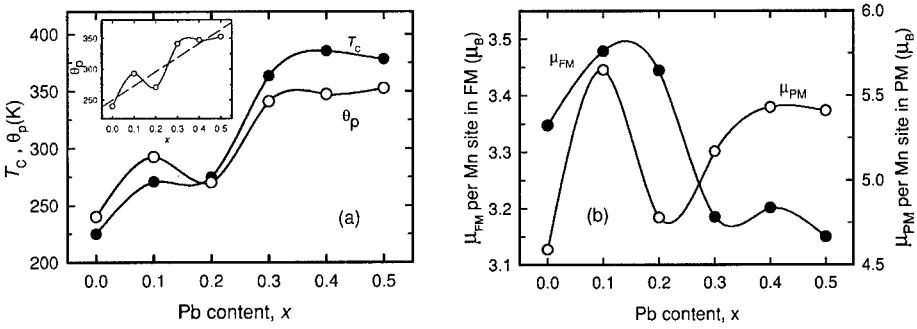

Figure 2. (a) Ferromagnetic and paramagnetic transition temperatures as a function of Pb content, $T_C(x)$ and $\theta_p(x)$. (b) Saturation and effective magnetic moments per Mn site *vs* Pb content. All curves serve as guide lines to the eyes.

For a well-defined magnetic phase transition the scaling theory [6-8] predicts that magnetic susceptibility χ, determined by the experimental $M(T)$ data in figure 3(a), exhibits a scaling relation as follows:

$$\chi - \chi_0 = \frac{C}{T-\theta_p}(1-q) = \frac{C}{T}[1-|t|^{\beta} f_{\pm}(H^2/|t|^{\beta+\gamma})], \quad (1)$$

$$q(t,H) = |t|^{\beta} f_{\pm}(H^2/|t|^{\beta+\gamma}), \quad (2)$$

$$q|t|^{-\beta} = f_{\pm}(H^2/|t|^{\beta+\gamma}), \quad (3)$$

where t is the reduced temperature $t = (T - T_0)/T_0$ with T_0 being certain transition temperature (T_C for a FM/PM transition or T_g for a SG transition). q is the order parameter as functions of T and H and the scaling functions f_+ and f_- apply for $t > 0$ (in PM phase) and $t < 0$ (in FM or SG phase),

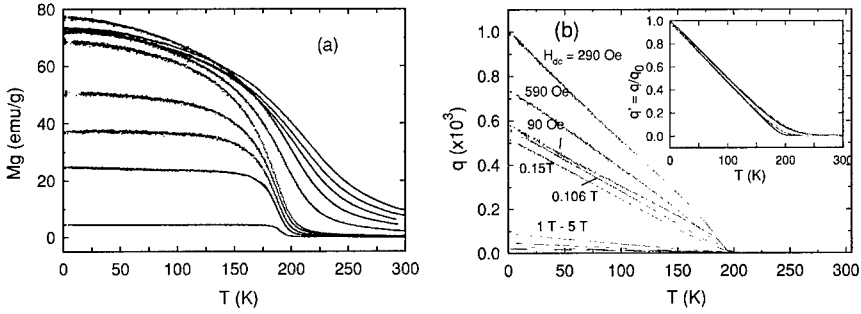

Figure 3. (a) Temperature dependence of FC magnetization, and (b) temperature dependence of order parameter of $LaMnO_3$ compound in 10 various applied fields: 0.009 - 5 T. The inset plot shows the normalized order parameter as a function of temperature.

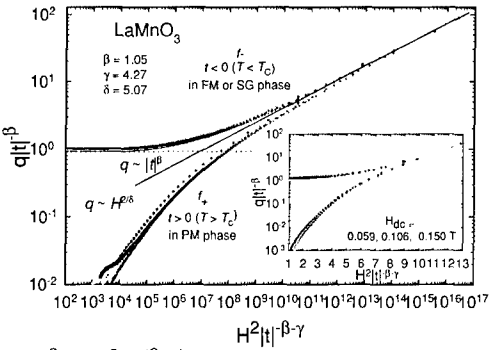

Figure 4. Log-log plot of $q|t|^{\beta}$ *vs* $H^2|t|^{-(\beta+\gamma)}$ of $LaMnO_3$ compound for data in H = 1, 2, 3, 4 and 5T. Inset plot shows the same plot for data in H = 0.059, 0.105 and 0.15 T. All data obtained in the ranges $2 \leq T \leq 305$ K collapse two scaling relation f_+ and f_- as Eq. (3).

respectively. For our $LaMnO_3$ sample, the values of the critical exponents $\beta = 1.05 \pm 0.1$, $\delta = 5.07 \pm 0.3$ and $\gamma = 4.3 \pm 0.5$ are derived by fitting $q(t) \sim q_0|t|^{\beta}$, $q(H) \sim q_0' H^{2/\delta}$ and $\delta = 1 + \gamma/\beta$. These exponents are similar to those found in conventional spin glasses. The β value is very close to the predicted value of the mean field theory, $\beta = 1$. Using these critical exponents, $C = 1.81 \times 10^{-2}$ cm^3/g·K, $\chi_0 = 0$ and $\theta_p = 213.3$ K all data of $M(T)$ in various fields give a plot of $q|t|^{-\beta}$ *vs* $H^2|t|^{-\beta-\gamma}$ shown in figure 3. All of the q data collapse onto two curves, that is, the scaling functions $f_+(x)$ for $t > 0$ ($T > T_0$, in the PM phase) and $f_-(x)$ for $t < 0$ ($T < T_0$, in the FM phase). For $t < 0$, $q|t|^{-\beta}$ approaches a constant (~ 1) for small $H^2|t|^{-\beta-\gamma}$ (the dashed line in figure 4). The solid line of $q \sim H^{2/\delta}$ with $\delta = 4.68$ in figure 4 demonstrates the asymptotic behavior for $T \rightarrow T_0$. The shapes of both the scaling functions are also quite similar to those observed in most conventional spin glasses.

ACKNOWLEDGMENTS

This work was supported by the National Science Council, R.O.C. under the grant No. NSC-89-2112-M194-023.

REFERENCES

1. J. M. D. Coey, M. Viret and S. von Molná, *Advances in Physics* **48**, 167 (1999).
2. C. Frontera, J. L. García-Muñoz, A. Llobet, M. Respaud, J. B. Broto, J. S. Lord and A. Planes, *Phys. Rev.* **B62**, 3381 (2000).
3. C. W. Searle and S. T. Wang, *Can. J. Phys.* **47**, 2703 (1969); **48**, 2023 (1970).
4. A. H. Morrish, B. J. Evans, J. A. Eaton and L. K. Leung, *Can. J. Phys.* **47**, 2691 (1969).
5. L. K. Leung, A. H. Morrish and C. W. Searle, *Can. J. Phys.* **47**, 2697 (1969).
6. F. C. Chou, N. R. Belk, M. A. Kastner, and R. J. Birgeneau and A. Aharony, *Phys. Rev. Lett.* **75**, 2204 (1995); B. Barbara, A. P. Malozemoff and Y. Imry, *Phy. Rev. Lett.* **47**, 1852 (1981).
7. A. P. Malozemoff, S. E. Barnes and B. Barbara, *Phy. Rev. Lett.* **51**, 1704 (1983).
8. N. Moutis, I. Panagiotopoulos, M. Pissas, and D. Niarchos, *Phys. Rev.* **B59**, 1129 (1999).